

A New Controlling Method for TRMS Based on Robust Approach

Mostafa Honari Torshizi¹, Javad Jahanpour*², Mohammadreza Gharib³

1- Master student, Islamic Azad University,
Mashhad Branch, mhonar2010@gmail.com

2- Assistant professor, Islamic Azad University, Mashhad Branch,
(Corresponding author: jahanpourfr@mshdiau.ac.ir)

3- PhD candidate, Ferdowsi University of Mashhad,
mech_gharib@yahoo.com

Paper Reference Number: 12516700

Name of the Presenter: Mostafa Honari Torshizi



Abstract

This paper provides a new method for control of a twin rotor multi-input multi-output system (TRMS), which it is named quantitative feedback theory (QFT). At first, the model of TRMS and differences/similarities in comparison with helicopter is introduced. The equations of motion by considering motion in both vertical and horizontal planes and relation between input and output of motors are obtained. The nonlinear TRMS is separated to two single input single output systems and state space equations for motion in each plane are presented. Then by linearization, the transfer functions for motion in each plane are achieved. Finally, using QFT method, controllers are designed for motion in each plane. Also, simulations for step-tracking have been carried out which indicates successful design of controllers and pre-filters.

Key words: QFT, Robust Control, State Space, TRMS.

1. Introduction

Vilchis (2003) stated that the main difficulties (at a theoretical level) for designing stable feedback controllers for helicopters stem from their nonlinearities and couplings (for the solid mechanics part) and the fact that the inputs are not torques nor forces but displacements of some elements which enter the dynamics through aerodynamical forces/torques. In certain aspects, TRMS behavior resembles that of a helicopter. The system is perceived as a challenging engineering problem due to its high nonlinearity, cross coupling between its two axes and inaccessibility of some of its states and outputs for measurements (Feedback Instruments Ltd. (1998), Juang, J.G. (2008), Pratab, B. (2010), Wen, P. (2008)). Accurate dynamic model of the system is required to be developed to achieve control objectives satisfactorily, and this is a more powerful motive issue to design a controller that can be able to control system with uncertainties, hence it is the QFT as a one of robust control method is selected. QFT has been introduced by Horowitz, which allows direct design to closed-loop robust performance and stability specifications. Consider the feedback system shown in diagram Fig.1. This system has two-degrees of freedom structure. In this diagram $p(s)$ is uncertain plant belongs to a set $p(s, \alpha)$, i.e. $p(s) \in \{p(s, \alpha); \alpha \in p\}$ where α is the vector of uncertain parameters for

uncertainty structured of $p(s)$, $G(s)$ is the fixed structure feedback controller and $F(s)$ is the prefilter (Horowitz, I. M. (1992), Amiri-M, A-A (2009)).

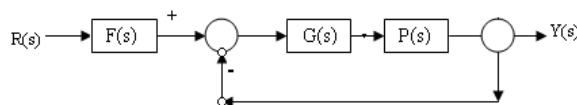


Fig 1: Structure of a two-degrees of freedom system.

2. Model Descriptions of the TRMS

The TRMS is a laboratory setup developed by Feedback Instrument Ltd. (Feedback Co. (1998)) for control experiments. It consists of a beam pivoted on its base in such a way that it can rotate freely both in its horizontal and vertical planes (Fig. 2). The TRMS has two degrees of freedom (DOF). At both end of the beam, there are two propellers driven by DC motors. The aerodynamic force is controlled by varying the speed of the motors. Therefore, the control inputs are the supplied voltages of the DC motors. The TRMS has main and tail rotors for generating vertical and horizontal propeller thrust. The main rotor produces a lifting force allowing the beam to rise vertically making a rotation around the pitch axis. While, the tail rotor is used to make the beam turn left or right around the yaw axis. Behavior of TRMS resembles that of a helicopter. For example, it possesses a strong cross coupling between the collective (main rotor) and the tail rotor, high nonlinearity, unstable and complex dynamics like a helicopter. However, the TRMS is substantially different from a helicopter. Table 1 lists the main differences between a helicopter and a TRMS (Rahideh, A. (2008)).

	TRMS	Helicopter
Location of pivot point	Midway between two rotors	The main rotor head
Lift generation or vertical control	Speed control of main rotor	Collective pitch control
Yaw is controlled by	Tail rotor speed	Pitch angle of the tail rotor blades
Cyclical control	No	Yes (for directional control)

Table 1. The main differences between a helicopter and a TRMS

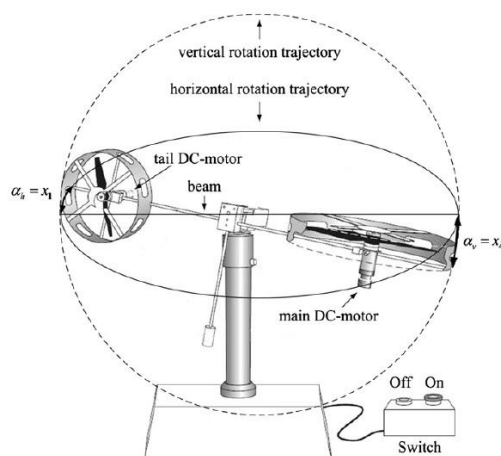


Fig 2: The twin rotor multi-input multi-output system (TRMS).

Writing Newton's second law of motion in vertical plane yields:

$$M_v = J_v \frac{d^2 \alpha_v}{dt^2} = \sum_{i=1}^4 M_{vi}, \quad J_v = \sum_{i=1}^8 J_{vi} \quad (1)$$

where, M_v is the total moment of forces in the vertical plane, J_v is the sum of moments of inertia relative to the horizontal axis and α_v is the pitch angle of the beam.

Considering Fig. 3, the moments of gravity forces can be calculated as following equation in which A, B and C are constant:

$$M_{v1} = g[(A - B) \cos \alpha_v - C \sin \alpha_v] \quad (2)$$

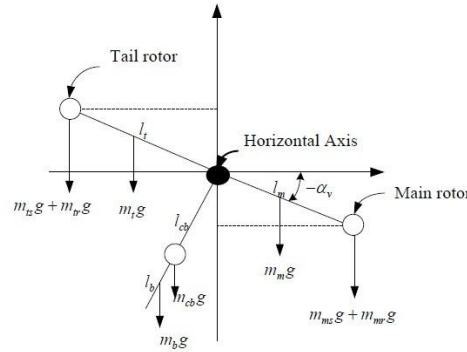


Fig 3: Gravity forces in TRMS corresponding to the return torque.

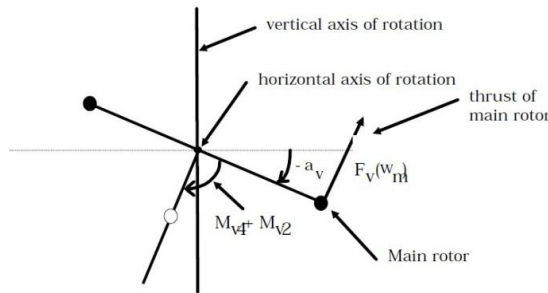


Fig 4: Propulsive force moment and friction moment in TRMS

Also, considering the situation shown in Fig. 4, the moments of propulsive forces applied to the beam is determined as follows:

$$M_{v2} = l_m F_v(\omega_m) \quad (3)$$

where, ω_m is the angular velocity of the main rotor and $F_v(\omega_m)$ denotes the dependence of the propulsive force on the angular velocity of the main rotor.

The moment of centrifugal forces corresponding to the motion of the beam around the vertical axis is:

$$M_{v3} = -\Omega_h^2 (A + B + C) \sin \alpha_v \cos \alpha_v \quad (4)$$

where, Ω_h is the angular velocity of the beam around the vertical axis, and α_h is the azimuth angle of the beam.

The moment of friction force depending on the angular velocity of the beam around the horizontal axis is:

$$M_{v4} = -\Omega_v k_v \quad (5)$$

where, Ω_v is the angular velocity around the horizontal axis and k_v is a constant.

Similarly, one can describe the motion of the beam in the horizontal plane (around the vertical axis) shown in fig 5. The driving torques is produced by the rotors and that the moment of inertia depends on the pitch angle of the beam.

$$M_h = J_h \frac{d^2 \alpha_h}{dt^2} = \sum_{i=1}^2 M_{hi}, \quad J_h = \sum_{i=1}^8 J_{hi} = D \cos^2 \alpha_v + E \sin^2 \alpha_v + F \quad (6)$$

where, M_h is the total moment of forces in the horizontal plane, J_h is the sum of moments of inertia relative to the horizontal axis, D, E and F are constant values.

To determine the moments of forces applied to the beam and making it rotate around the vertical axis consider the situation shown in Fig. 5 and we have:

$$M_{h1} = l_t F_h(\omega_t) \cos \alpha_v \quad (7)$$

where, ω_t is the angular velocity of the tail rotor and $F_h(\omega_t)$ denotes the dependence of the propulsive force on the angular velocity of the tail rotor.

The moment of friction depending on the angular velocity of the beam around the vertical axis is:

$$M_{h2} = -\Omega_h k_h \quad (8)$$

where, k_h is constant.

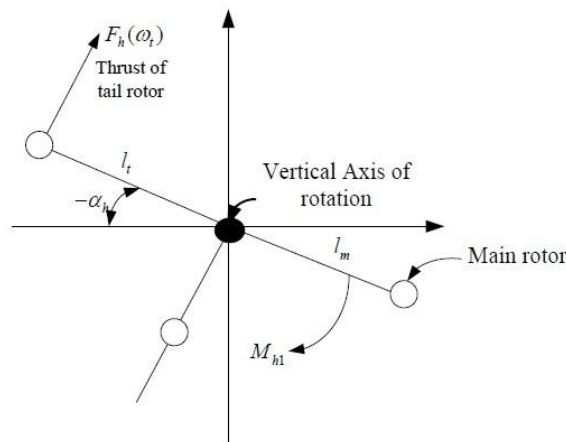


Fig 5: Moments of forces in horizontal plane (as seen from above)

3. State space equations

Using (1)-(5) we can write the equations describing the motion of the system in vertical plane as follows:

$$\frac{dS_v}{dt} = l_m S_f F_v(\omega_m) - \Omega_v k_v + g((A - B) \cos \alpha_v - C \sin \alpha_v) - \frac{1}{2} \Omega_h^2 (A + B + C) \sin 2\alpha_v \quad (9)$$

$$\frac{d\alpha_v}{dt} = \Omega_v = S_v + \frac{J_{tr} \omega_t}{J_v} \quad (10)$$

where, S_v is the angular momentum in vertical plane for the beam, S_f is the balance scale, and J_{tr} is the moment of inertia in DC-motor -tail propeller subsystem.

Using (6)-(8) we can write the equations describing the motion of the system in horizontal plane as follows:

$$\frac{dS_h}{dt} = l_t S_f F_h(\omega_t) \cos \alpha_v - \Omega_h k_h \quad (11)$$

$$\frac{d\alpha_h}{dt} = \Omega_h = \frac{S_h J_{mr} \omega_m \cos \alpha_v}{J_h} \quad (12)$$

where, S_h is the angular momentum in horizontal plane for the beam and J_{mr} is the moment of inertia in DC-motor -main propeller subsystem.

It should be noted that angular velocities are nonlinear functions of the input voltage of the DC-motor. Thus we have two additional equations:

$$\frac{du_{vv}}{dt} = \frac{1}{T_{mr}} (-u_{vv} + u_v) \quad (13)$$

$$\frac{du_{hh}}{dt} = \frac{1}{T_{tr}} (-u_{hh} + u_h) \quad (14)$$

where, u_{vv} is the output of the main DC motor, u_{hh} is the output of the tail DC motor, T_{mr} is the time constant of main motor propeller system and T_{tr} is the time constant of tail motor propeller system.

Two nonlinear input characteristics determine dependence of DC-motor rotational speed on input voltage ($\omega_m = P_v(u_{vv}), \omega_t = P_h(u_{hh})$) and two nonlinear characteristics determine dependence of propeller thrust on DC-motor rotational speeds ($F_v = F_v(\omega_m), F_h = F_h(\omega_t)$). For characterizing nonlinear functions ω_m, ω_t, F_v and F_h , experimental results in Feedback Instruments Ltd. (1998) have been employed that they are:

$$\omega_m = 90.99u_{vv}^6 + 599.73u_{vv}^5 - 129.26u_{vv}^4 - 1238.64u_{vv}^3 + 63.45u_{vv}^2 + 1283.4u_{vv} \quad (15)$$

$$\omega_t = 2020u_{hh}^5 - 194.69u_{hh}^4 - 4283.15u_{hh}^3 + 262.27u_{hh}^2 + 3796.83u_{hh} \quad (16)$$

$$F_v = -3.48 \times 10^{-12} \omega_m^5 + 1.09 \times 10^{-9} \omega_m^4 + 4.123 \times 10^{-6} \omega_m^3 - 1.632 \times 10^{-4} \omega_m^2 + 9.544 \times 10^{-2} \omega_m \quad (17)$$

$$F_h = -3 \times 10^{-14} \omega_t^5 - 1.595 \times 10^{-11} \omega_t^4 + 2.511 \times 10^{-7} \omega_t^3 - 1.808 \times 10^{-4} \omega_t^2 + 0.0801 \omega_t \quad (18)$$

Now by use of previous equations and after decoupling, the state space equations are:

$$\begin{aligned} \dot{x}_1 &= x_2 \\ \dot{x}_2 &= 9.1[l_m S_f F_v(\omega_m) - k_v x_2 - g(0.0099 \cos x_1 + 0.0168 \sin x_1) \\ &\quad - 0.0252 x_5^2 \sin 2x_1 + J_{tr} \dot{\omega}_t (u_h - x_6) / T_{tr}] \\ \dot{x}_3 &= (u_v - x_3) / T_{mr} \\ \dot{x}_4 &= x_5 \\ \dot{x}_5 &= \frac{l_t S_f F_h(\omega_t) \cos x_1 - k_h x_5 - x_5 x_1 (E - F) \sin 2x_1}{D \cos^2 x_1 + E \sin^2 x_1 + F} \\ &\quad + \frac{J_{mr} \omega_m x_2 \sin x_1 + J_{mr} \dot{\omega}_m (u_v - x_3) / T_{tr}}{D \cos^2 x_1 + E \sin^2 x_1 + F} \\ \dot{x}_6 &= (u_h - x_6) / T_{tr} \end{aligned} \quad (19)$$

where, $x_v = [x_1 \ x_2 \ x_3] = [\alpha_v \ \Omega_v \ u_{vv}]$ is the state vector for the vertical subsystem, and $x_h = [x_4 \ x_5 \ x_6] = [\alpha_h \ \Omega_h \ u_{hh}]$ is the state vector for the horizontal subsystem. Furthermore $[u_v \ u_h]$ and $[\alpha_v \ \alpha_h]$ are the input and output vectors, respectively.

4. Gaining Transfer Functions and Designing Robust Control for the TRMS

Before gaining the transfer functions, the previous nonlinear functions must be linearized. For this job, the method which has been used in (Taoa, C.W. (2010).) is used. The linear state equations for motion in both planes are:

$$\dot{x}_v = \sum_{i=1}^2 h_{vi} f_{vi}(x_v, u_v) \quad (20)$$

$$\dot{x}_h = \sum_{i=1}^2 h_{hi} f_{hi}(x_h, u_h) \quad (21)$$

where:

$$f_{v1}(x_v, u_v) = \begin{bmatrix} x_2 \\ 9.1[l_m S_{fL_{v1}} - k_v x_2 - g(0.0099 \cos x_1 + 0.0168 \sin x_1) \\ - 0.0252 x_5^2 \sin 2x_1 + J_{tr} \dot{\omega}_t (u_h - x_6) / T_{tr}] \\ (u_v - x_3) / T_{mr} \end{bmatrix} \quad (22)$$

$$f_{v2}(x_v, u_v) = \begin{bmatrix} x_2 \\ 9.1[l_m S_{fL_{v2}} - k_v x_2 - g(0.0099 \cos x_1 + 0.0168 \sin x_1) \\ - 0.0252 x_5^2 \sin 2x_1 + J_{tr} \dot{\omega}_t (u_h - x_6) / T_{tr}] \\ (u_v - x_3) / T_{mr} \end{bmatrix} \quad (23)$$

$$f_{h1}(x_h, u_h) = \begin{bmatrix} x_5 \\ \frac{l_t S_{fL_{h1}} \cos x_1 - k_h x_5 - x_5 x_1 (E - F) \sin 2x_1}{J_h} \\ + \frac{J_{mr} \omega_m x_2 \sin x_1 + J_{mr} \dot{\omega}_m (u_v - x_3) / T_{tr}}{J_h} \\ (u_h - x_6) / T_{tr} \end{bmatrix} \quad (24)$$

$$f_{h2}(x_h, u_h) = \begin{bmatrix} x_5 \\ \frac{l_t S_{fL_{h2}} \cos x_1 - k_h x_5 - x_5 x_1 (E - F) \sin 2x_1}{J_h} \\ + \frac{J_{mr} \omega_m x_2 \sin x_1 + J_{mr} \dot{\omega}_m (u_v - x_3) / T_{tr}}{J_h} \\ (u_h - x_6) / T_{tr} \end{bmatrix} \quad (25)$$

$$L_{v1} = 810x_3 + 500, \quad L_{v2} = 720x_3 - 500 \quad (26)$$

$$L_{h1} = 575x_6 + 300, \quad L_{h2} = 850x_6 - 800 \quad (27)$$

Also, h_{hi} and h_{vi} are weight factors.

By use of previous linearized state space equations and using numerical data from (Feedback Instruments Ltd. (1998), Taoa, C.W. (2010).), the transfer functions are as follows:

$$G_v = \frac{\alpha_v(s)}{u_v(s)} = \frac{a_v}{s^3 + 0.73s^2 + b_v s + 3.972} \quad (28)$$

$$G_h = \frac{\alpha_h(s)}{u_h(s)} = \frac{a_h}{s^3 + 3.47s^2 + b_h s} \quad (29)$$

where, $0.4 \leq a_v \leq 1.6$, $13 \leq a_h \leq 22$, $1.5 \leq b_v \leq 5.8$, and $2 \leq b_h \leq 3$ are the range of coefficients (uncertainties) which come from the varying of α_v and α_h .

The overshoot and the rise time specifications ($M_p = 25\%$) and ($t_r = 5$ s) respectively are given in the form of upper ($a(\omega)$) and lower ($b(\omega)$) bounds in frequency domain, usually based on simple second-order models to represent the status of damped condition (Amiri-M, A-A., (2009)).

$$a(\omega) < F(j\omega) \frac{G(j\omega)K(j\omega)}{1 + G(j\omega)K(j\omega)} < b(\omega) \quad (30)$$

5. Results and Analysis

By using the elements of the QFT toolbox one can design the controller so that the open loop transfer function exactly lies on its robust performance bounds and does not penetrate the U-contour at all frequency values (ω_i). The design of pre-filter guarantees the

satisfaction of tracking specification. In Figs. 6 and 7, Loop and Pre-Filter Shaping of open loop transfer function for vertical motion are shown.

To summarize the paper, the controller designing steps are just illustrated for vertical motion in this paper.

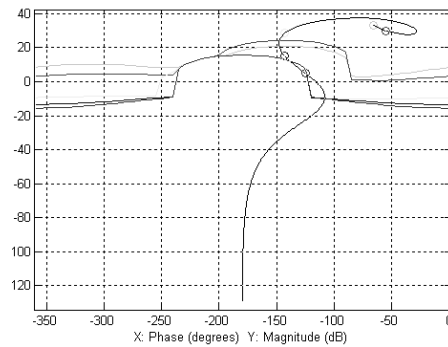


Fig 6: Loop-shaping in Nichols chart for vertical motion

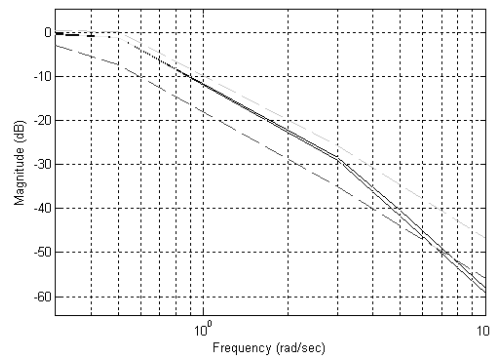


Fig 7: Pre-Filter Shaping in Nichols Chart for vertical motion

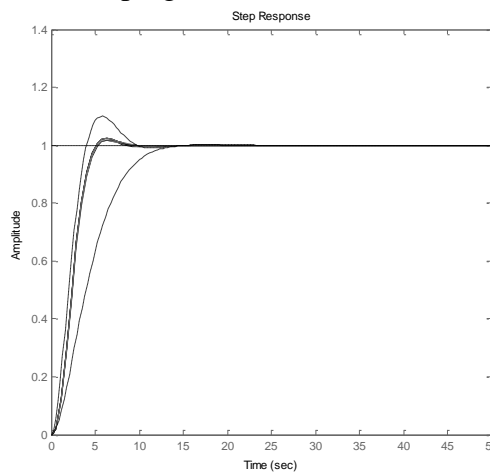


Fig 8: Step Response and Control Effort of System for vertical motion

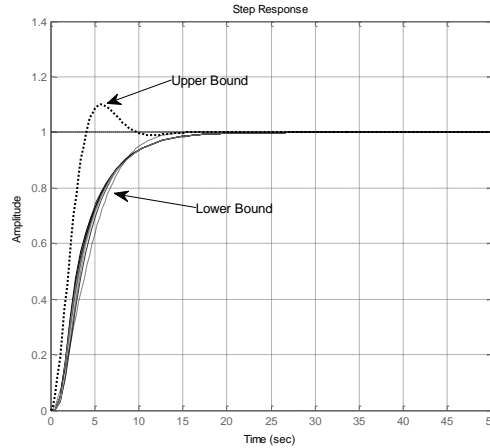


Fig 9: Step Response and Control Effort of System for horizontal motion

The respected controller and prefilter for vertical and horizontal motion are found respectively as:

$$K_v(s) = \frac{8.8 \times 10^3 s^3 + 6.3 \times 10^4 s^2 + 5.5 \times 10^4 s + 7.15 \times 10^3}{s^2 + 248.6s} \quad (31)$$

$$K_h(s) = \frac{0.244s^2 + 0.354s + 0.128}{s + 0.32} \quad (32)$$

$$F_v(s) = \frac{1.121}{s^3 + 1.21s^2 - 0.844s + 1.22} \quad (33)$$

$$F_h(s) = \frac{0.29}{s^3 + 0.29s^2 + 7.91s + 2.29} \quad (34)$$

The time domain closed loop response of vertical and horizontal motion including controller and pre-filter are shown in Figs.8 and 9, respectively which indicates the design is accurate.

6. Conclusions

In this paper, dynamic model of TRMS for motion in both vertical and horizontal planes have been introduced. The state space equations of motion for the presented dynamic model of TRMS have been decoupled and linearized. Also, employing QFT approach, the new algorithm for designing controller for the TRMS has been proposed. The simulation results for step- tracking problem in vertical and horizontal planes indicate Successful implementation of robust controller design for TRMS motion.

References

- Amiri-M, A-A., Gharib, M.R, & Moavenian, M. (2009). Modeling and Control of a SCARA Robot Using Quantitative Feedback Theory. Proc. IMechE Part I: *J. Systems and Control Engineering*. 223.
- Feedback Instruments Ltd. (1998). *Twin Rotor MIMO System 33-007-4M5 User Manual*. East Sussex, U.K.
- Horowitz, I. M. (1992). *Quantitative Feedback Design Theory (QFT)*. 1, QFT Publications, 4470 Grinnel Ave., Boulder, Colorado 80303, USA.
- Juang, J.G., Lin, R.W, & Liu W.K. (2008). Comparison of classical control and intelligent control for a MIMO system. *Applied Mathematics and Computation*. 205, 778–791.

Pratab, B., & Purwar, S. (2010). Neural Network Observer for Twin Rotor MIMO System: An LMI Based Approach. In *Proceedings of the 2010 International Conference on Modelling, Identification and Control*. Okayama, Japan, July 17-19, 539-544.

Rahideh, A., Shaheed, M.H., & Huijberts, H.J.C. (2008). Dynamic modelling of a TRMS using analytical and empirical approaches. *Control Engineering Practice*. 16, 241–259.

Taoa, C.W., Taurb, J.S., & Chena, Y.C. (2010). Design of a parallel distributed fuzzy LQR controller for the twin rotor multi-input multi-output system. *Fuzzy Sets and Systems*. 161, 2081–2103.

Vilchis, J.C.A., Brogliato, B., Dzul, A., & Lozano, R. (2003). Nonlinear modeling and control of helicopters. *Automatica*. 39(9), 1583-1596.

Wen, P., & Lu, T.W. (2008). Decoupling control of a twin rotor MIMO system using robust deadbeat control technique. *IET control theory applications*. 2(11), 999-1007.